Myocardial BDNF regulates cardiac bioenergetics through the transcription factor Yin Yang 1

Xue Yang[1,2 †], Manling Zhang[1,3 †*], Raymond J. Zimmerman[1], Qin Wang[1,4], An-chi Wei [5,6], Guangshuo Zhu [6], Djahida Bedja [6], Hong Jiang[3], Sruti S. Shiva[1], Iain Scott[1], Brian O'Rourke[6], David A. Kass[6], Nazareno Paolocci[6], Ning Feng [1,2*]

† Equal contribution

*Correspondence: Manling Zhang MD, MS

Department of Medicine, Division of Cardiology

Vascular Medicine Institute

University of Pittsburgh

200 Lothrop St, PUB C702

Pittsburgh, PA 15213

Email: Zhangm5@upmc.edu

Tel: 412-383-9054

*Correspondence: Ning Feng MD, PhD

Department of Medicine, Division of Cardiology

Vascular Medicine Institute

University of Pittsburgh

203 Lothrop St, Biomedical Sciences Tower, E 1245

Pittsburgh, PA 15213

Email: fengn@pitt.edu, or fengn@upmc.edu

Tel: 412-383-2835

1. Department of Medicine, Division of Cardiology, Vascular Medicine Institute, University of Pittsburgh, Pittsburgh, PA 15213
2. Department of Cardiology, Zhongshan Hospital, Fudan University, Shanghai, China
3. Division of Cardiology, Veteran Affair Pittsburgh Healthcare System, Pittsburgh, PA, 15213
4. Echocardiography lab at Heart Center, Ningxia General Hospital, Ningxia Medical University, Ningxia, China
5. Department of Electrical Engineering, Graduate Institute of Biomedical and Bioinformatics, National Taiwan University, Taiwan
6. Division of Cardiology, Department of Medicine, Johns Hopkins University, Baltimore, MD 20215

Conflict of interest: The authors have declared that no conflict of interest exists.

ABSTRACT

Serum Brain-derived Neurotrophic Factor (BDNF) is markedly decreased in heart failure patients. Both BDNF and its receptor, Tropomyosin Related Kinase Receptor (TrkB), are expressed in cardiomyocytes, however the role of myocardial BDNF signaling in cardiac pathophysiology is poorly understood. We found that myocardial BDNF expression was increased in mice with swimming exercise, but decreased in a mouse heart failure model. Cardiac-specific TrkB knockout (cTrkB KO) mice displayed a blunted adaptive cardiac response to exercise, with attenuated upregulation of transcription factor networks controlling mitochondrial biogenesis/metabolism, including Peroxisome proliferator-activated receptor gamma coactivator 1 alpha (PGC-1α). In response to pathological stress (transaortic constriction, TAC), cTrkB KO mice showed an exacerbated heart failure progression. The expression of PGC-1α and other metabolic transcription factors were downregulated in cTrkB KO mice exposed to TAC. Consistent with this, mitochondrial DNA copy number and mitochondrial protein abundance was markedly decreased in cTrkB KO mice, resulting in decreased mitochondrial respiratory function. We further unraveled that BDNF induces PGC-1α upregulation and bioenergetics through a novel signaling pathway, the pleiotropic transcription factor Yin Yang 1 (YY1). Taken together, our findings suggest that myocardial BDNF plays a critical role in regulating cellular energetics in the cardiac stress response.

INTRODUCTION

Endurance exercise has long been linked to cardiovascular health. Multiple recent large-scale prospective or retrospective studies demonstrated that exercise, and the intensity of exercise, is inversely associated with long-term all-cause mortality and CVD mortality (1-3). Heart failure is a major public health challenge with high mortality and cost. Exercise training and cardiac rehabilitation have demonstrated numerous benefits for people with heart failure, including improved exercise capacity, increased quality of life, reduced hospitalization, and even decreased mortality rate (4-6). Recently launched guidelines for the diagnosis and treatment of acute and chronic heart failure have incorporated a recommendation for regular aerobic exercise in patients with heart failure (7, 8). However, the molecular mechanism underlying exercise benefits on heart health are still poorly understood, and are pivotal for the development of novel heart failure therapies.

Brain-derived neurotrophic factor (BDNF) is a neurotrophin that regulates energy homeostasis, mitochondrial bioenergetics, and mediates exercise-induced neurogenesis in the brain (9). In a prospective study using the Framingham Heart Study cohort, it was found that circulating BDNF levels are inversely associated with the risk of cardiovascular disease (10). In addition, retrospective studies show that decreased levels of circulating BDNF are associated with heart failure, worse functional status, higher NT-proBNP, and mortality (11-13). BDNF and its receptor, Tropomyosin related kinase receptor B (TrkB), were found in myocardium (14), but little is known about the role of myocardial BDNF signaling in cardiac pathophysiology. Our previous study revealed that myocardial BDNF/TrkB signaling is crucial for optimal excitation-contraction coupling (14). BDNF has

been reported to promote cardiomyocyte survival in myocardial ischemic-reperfusion injury (15). Given the emerging evidence that BDNF regulates energy homeostasis in brain and peripheral tissues (9), we investigated whether myocardial BDNF/TrkB signaling has any impact on cardiac bioenergetics in response to pathophysiological stress. We found that myocardial BDNF signaling plays a critical role in cardiac bioenergetic regulation in response to exercise or pathological stress, and that upregulation of PGC-1α and other metabolic transcription factors expression appears to be a key underlying mechanism.

RESULTS

BDNF expression in heart is increased with endurance exercise but decreased in failing hearts

To determine the importance of BDNF signaling in the cardiac response to physiological stimuli or pathological stress, myocardial BDNF expression was examined in C57BL/6J mice subjected to swimming exercise or transaortic constriction (TAC). BDNF expression in the heart was significantly increased in C57BL/6J mice subjected to swimming exercise compared to sedentary littermate controls (Fig 1A). Consistently, the phosphorylation of TrkB, the marker of TrkB activation upon BDNF binding, was also increased with swimming exercise (Fig 1A). In contrast, cardiac BDNF expression and levels of phosphorylated TrkB were decreased in the pressure overload-induced failing hearts (Fig 1B). These findings suggest that myocardial BDNF signaling may play a critical role in cardiac adaptive response to endurance exercise, and impaired BDNF signaling may be an important mechanism for heart failure.

Cardiac-specific TrkB KO mice show exacerbated heart failure progression against pressure overload

To determine whether impaired myocardial BDNF signaling plays a role in heart failure progression, both male and female cardiac-specific TrkB KO mice (cTrkB KO) were subjected to TAC. TrkB is primarily the receptor for BDNF, though TrkB could also bind Neurotrophin 4 (NT-4). The cardiac-specific TrkB KO mice instead of cardiac-specific BDNF KO mice were selected for this study because it is unclear whether cardiomyocytes derived BDNF is the main resource of BDNF in the heart. It is also unclear whether

circulating BDNF has an impact on cardiomyocytes. Compared to WT littermate controls, male cTrkB KO mice began to display worse cardiac function at 10 days post TAC. Cardiac function in male cTrkB KO mice further deteriorated at 6 weeks post-TAC with decreased fractional shortening (WT 40.02±2.7% [n=22] vs. cTrkB KO 23.1±2.1% [n=15], *P<0.0001*) (Fig 2A, B), increased dilation of left ventricular chamber (Fig 2A, B), increased heart weight and lung weight (Fig 2C), and augmented fetal gene reprogramming (Fig 2D). Consistent with this, female cTrkB KO mice showed accelerated heart failure progression after TAC compared to WT controls (Fig S1). Taken together, our findings showed that myocardial BDNF signaling is essential to protect the heart against pathological stress.

PGC-1α and metabolic transcription factors are markedly decreased in cTrkB KO mice subjected to TAC

One prominent feature of late stage heart failure is profound metabolism remodeling, characterized by decreased cardiac ATP or energy production resulted from diminished oxidative phosphorylation and compromised mitochondrial biogenesis(16). The metabolic derangement is likely the consequence of repressed transcription factor networks controlling metabolic genes transcription. Peroxisome proliferator activated receptor gamma coactivator 1 alpha (PGC-1α), the master regulator of metabolic genes and mitochondrial biogenesis is markedly suppressed in heart failure(17). Cardiac PGC-1α exerts its pleiotropic actions through direct interaction with, or activation of a network of, nuclear transcription factors (18). PGC-1α activates Peroxisome proliferator-activated receptor α (PPARα) to regulate fatty acid oxidation (19, 20). PGC-1α promotes mitochondrial biogenesis and mitochondrial metabolism through its interaction with

Estrogen-related receptor α (ERRα) and mitochondrial transcription factor A (TFAM)(21). Given that BDNF regulates PGC-1α and energetics in the brain(22), we next investigated whether the regulation of PGC-1α by BDNF is also critical in the cardiac response to pathological stress. We observed that PGC-1α, along with other metabolic transcription factors such as PPARα, ERRα, and TFAM, were significantly decreased in TAC cTrkB KO mice hearts compared to WT controls, suggesting myocardial BDNF was essential in regulating cardiac metabolism in response to pathological stress (Fig 3A, B).

Mitochondrial DNA copy number, protein level and function are significantly reduced in cTrkB KO mice subjected to TAC

We next examined whether downregulation of PGC-1α and the other nuclear transcription factors resulted in reduced mitochondrial biogenesis/content, and impaired mitochondrial respiratory function in cTrkB KO mice. Mitochondrial protein abundance was assessed by Oxphos Western Blot cocktail antibodies. ATP Synthase F1 Subunit Epsilon (ATP5A), Ubiquinol-Cytochrome C Reductase Core Protein 2 (UQCRC2), mitochondrially-encoded Cytochrome C Oxidase II (COXII), Succinate Dehydrogenase Complex Iron Sulfur Subunit B CSDHB), and NADH:Ubiquinone Oxidoreductase Subunit B8 (NDUFB8) were all significantly decreased in cTrkB KO mice subjected to TAC (Fig 4A). Mitochondrial biogenesis was assessed by mitochondrial DNA (Mitochondrially Encoded NADH:Ubiquinone Oxidoreductase Core Subunit 2, MT-ND2, or Mitochondrially Encoded ATP Synthase Membrane Subunit 6, MT-ATP6) to genomic DNA (18s RNA) ratio. In our experimental model, at the point of heart harvest, mitochondrial DNA copy number was increased in WT controls subjected to TAC. Relative to WT controls, mitochondrial DNA copy number was markedly decreased in stressed cTrkB KO mice

hearts (Fig 4B). In addition, we evaluated mitochondrial respiratory function on freshly isolated mitochondria in TAC cTrkB KO mice using the Seahorse XF Bioanalyzer. Complex II and complex IV oxygen consumption rate (OCR) were significantly decreased in cTrkB KO mice subjected to TAC (Fig 4C), while Complex I OCR was preserved (Fig S2). Collectively, consistent with markedly downregulated energy-related nuclear transcription factors, mitochondrial function, content, and biogenesis were impaired in cTrkB KO mice subjected to TAC.

Myocardial BDNF regulates PGC-1α expression through AKT-Raptor-YY1 pathway

We investigated the signaling pathways mediating BDNF-induced PGC-1α expression. It has been reported that Erk/CREB mediates BDNF-induced PGC-1α upregulation in the brain(22). However, there was little change in CREB activation in cTrkB KO mice subjected to TAC, and the Erk level was increased in TAC cTrkB KO mice (Fig S3A). In addition, chromatin immunoprecipitation assay (ChIP) showed there is no difference in the binding of CREB to PGC-1α promotor between WT and cTrkB KO mice subjected to TAC (Fig S3B). AMPK, an important regulator of PGC-1α, is implicated in BDNF induced fatty acid oxidation enhancement in skeletal muscle responding to contraction(23). We therefore investigated whether AMPK is involved in BDNF-induced PGC-1α upregulation in the heart, but found that there was little change of phosphorylated or total AMPK level in cTrkB KO mice subjected to TAC (Fig S3A). Instead, we found that phosphorylated AKT (p-AKT) was markedly decreased in cTrkB KO mice subjected to TAC, without significant change in total AKT level (t-AKT) (Fig 5A). AKT/mTOR is a common downstream signaling pathway of growth factor/tyrosine kinase receptors, and it was reported that mTOR coordinates cellular growth and energy metabolism by

controlling PGC-1α and other metabolic gene transcription (24). The mTOR regulates PGC-1α expression by promoting Yin Yang transcription factor 1 (YY1) and Raptor binding to the PGC-1α promoter(24). We therefore investigated whether AKT/mTOR/YY1/Raptor is involved in BDNF-induced PGC-1α expression. We found that YY1 was significantly increased in WT mice subjected to TAC, however, the upregulation of YY1 was blunted in cTrkB KO mice (Fig 5A). Surprisingly, we found there was no change in either phosphorylated mTOR (p-mTOR) at serine 2448 site, or total mTOR (t-mTOR) in cTrkB KO mice subjected to TAC (Fig S3C). In addition, there was no change in either phosphorylated Tuberous Sclerosis Complex 2 (p-TSC2) at threonine 1462 or total TSC2 (t-TSC2) levels, a key regulator of mTOR and an immediate downstream target of AKT(25), in cTrkB KO mice subjected to TAC (Fig S3C). Serine 2448 in mTOR and threonine 1462 in TSC2 are known to be targeted by AKT. However, given AKT has multiple phosphorylation sites on these two proteins, it is still quite possible that BDNF elicited AKT activation modulates mTOR or TSC2 activity through phosphorylation. There was also no difference in Raptor expression between WT controls and cTrkB KO mice (Fig S3C). However co-immunoprecipitation studies revealed that binding of YY1 with Raptor was decreased in cTrkB KO mice subjected to TAC compared to WT mice (Fig 5B). Taken together, our findings suggest that BDNF controls PGC-1α expression through AKT activation and the promotion of YY1-Raptor complex formation.

TrkB knockdown in NRCM decreases PGC-1α expression

To further demonstrate that YY1 is the key mediator of BDNF regulating PGC-1α expression, TrkB was knocked down with siRNA in neonatal rat cardiomyocytes (NRCMs). The efficiency of knockdown was validated by RT-PCR (Fig S4). We found that β-

adrenergic stimulation with isoproterenol increased BDNF expression (Fig 6A). Consistent with the *in vivo* studies, we found TrkB knockdown attenuated isoproterenol-induced AKT phosphorylation, YY1 and PGC-1α upregulation, suggesting AKT-YY1 is implicated in BDNF regulation on PGC-1α expression (Fig 6B). Moreover, we showed the binding of YY1 to PGC-1α promoter was decreased with TrkB knockdown using chromatin immunoprecipitation assay (ChIP). (Fig 6C). Because YY1 could be either transcription activator or repressor(26), we examined whether YY1 promotes PGC-1α transcription in cardiac myocytes. Indeed, YY1 knockdown decreased PGC-1α expression in NRCMs with or without isoproterenol stimulation (Fig 6D). Importantly, overexpression of YY1 recovered the downregulation of PGC-1α expression in cardiomyocytes with TrkB knockdown, demonstrating YY1 is the key mediator of BDNF regulation on PGC-1α expression (Fig 6E). Therefore, our study provided a new downstream signaling pathway of BDNF signaling.

TrkB knockdown in NRCM impairs mitochondrial function

To determine whether there is a functional consequence of decreased PGC-1 expression in the NRCMs with TrkB and YY1 knockdown, we investigated the mitochondrial function in NRCMs with TrkB and YY1 knockdown using Seahorse XF system (Seahorse Bioscience). Without isoproterenol stimulation, there was no difference in oxidative respiratory capacity in NRCMs with TrkB knockdown, but the oxygen consumption rate was significantly decreased in NRCMs with TrkB knockdown at basal respiratory condition in the presence of isoproterenol (Fig 7A). With YY1 knockdown, the oxidative respiratory capacity was markedly decreased under both basal condition and maximum capacity, with and without isoproterenol stimulation (Fig 7B), indicating YY1

plays an essential role in regulating bioenergetics in cardiac myocytes. These findings revealed a new role of YY1 in the heart.

cTrkB KO mice display blunted adaptive response to exercise

The chronic exercise-induced cardiac adaptive response protects the heart against pathological stress (27). Upregulation of PGC-1α expression and other metabolic transcription factors, including PPARα, ERRα, and TFAM, is at the center of adaptive response (28, 29). To determine if BDNF/TrkB signaling plays a role in the cardiac adaptive response to exercise, cTrkB KO mice were subjected to swimming exercise. We found that while exercise induced increased PGC-1α, PPARα, ERRα, and TFAM expression in WT mice, but the upregulation of these metabolic transcription factors was blunted in cTrkB KO mice (Fig 8A). These findings suggested that myocardial BDNF signaling plays a critical role in cardiac adaptive response to endurance exercise.

We further investigated whether AKT-YY1 is also responsible for BDNF-induced PGC-1α upregulation in response to exercise. Similarly to the TAC response, we found there is no significant difference in phosphorylated and total Erk, CREB, AMPK, mTOR, and TSC2 between WT and cTrkB KO mice subjected to swimming exercise (Fig S5). We showed p-AKT and YY1 were increased with swimming exercise, but the upregulation of p-AKT and YY1 responding to exercise was blunted in cTrkB KO mice (Fig 8B), indicating AKT-YY1 plays an essential role in BDNF-induced PGC-1α transcription in response to both exercise and pathological stress.

DISCUSSION

The role of myocardial BDNF signaling in cardiac pathophysiology is poorly understood. Here, we showed that myocardial BDNF signaling was enhanced in response to endurance exercise but was impaired in failing hearts. Using cardiac-specific TrkB KO model, we demonstrated that myocardial BDNF signaling played an essential role in the adaptive response to exercise, and protected against heart failure progression induced by chronic hemodynamic stress. Our findings suggested myocardial BDNF signaling controlled the abundance of cardiac metabolic transcription regulators including PGC-1α, PPARα, ERRα, and TFAM in response to exercise and pathological stress. These findings suggest that myocardial BDNF signaling-elicited bioenergetics enhancement may be one of the underlying molecular mechanisms in the exercise-induced adaptive response and exercise-granted cardiovascular protection. Developing therapeutic drugs targeting the BDNF signaling pathway may provide exercise-mimic beneficial effects against pathological stress, especially for patients with limited exercise capacity. The therapeutic approach targeting BDNF signaling, thereby targeting cardiac metabolism/bioenergetics, differs from standard heart failure therapy aiming at neurohormone inhibition, and therefore has the potential to provide additional or synergistic benefit for heart failure patients who are already on standard therapies. Because impaired BDNF signaling plays a critical role in many neurodegerative diseases, there has long been a major interest to develop TrkB agonists. Currently there are a number of small molecular compounds or peptide-based TrkB agonists proven effective in animal models of neurodegenerative diseases (30-32). Our findings suggest these TrkB agonists could be potentially repurposed for heart failure therapy.

We observed that BDNF expression is increased in the heart in response to exercise. However, which cell type is responsible for this enhanced BDNF level in heart remains unclear, since BDNF is expressed in nerves (15), vascular endothelial cells (33) and vascular smooth muscle cells, and cardiac myocytes (14, 15). Our cultured cardiac myocytes studies suggested paracrine or autocrine of BDNF in the cardiomyocytes may at least play some role. In contrast to exercise, we found chronic hemodynamic stress results in decreased BDNF expression in the heart. The molecular mechanism of this decreased BDNF expression is unclear. BDNF expression is also decreased in neurodegenerative diseases (34), and two mechanisms are often involved in this impairment. One mechanism is increased methylation of the BDNF promotor, which leads to enhanced binding of MeCP2, a transcriptional suppressor, to the BDNF promotor (35). Another mechanism of BDNF downregulation is increased miR-212/132 binding to 3' UTR of BDNF mRNA (36). Enhanced MeCP2 and miR-212/132 signaling have been reported to play an important role in cardiac hypertrophy (37, 38). Whether these two mechanisms of BDNF suppression are also involved in the failing heart needs to be investigated.

Our study provided one new downstream signaling pathway mediates BDNF action. We found that cardiac BDNF signaling activated AKT, promoting raptor/YY1 complex formation in response to pathophysiological stress. YY1 expression in the heart was increased with exercise or TAC, but the upregulation was attenuated in cTrkB KO mice. Consistently, in cultured cardiomyocytes, knockdown of TrkB attenuated β-adrenergic stimulation induced YY1 and PGC-1α upregulation, and the binding of YY1 to PGC-1α promoter. Importantly, YY1 overexpression rescued TrkB knockdown induced PGC-1α downregulation, demonstrating YY1 is the key mediator of BDNF induced PGC-

1α expression. YY1 is a multifunctional transcription factor that can act as a transcriptional repressor, a transcriptional activator, or a transcriptional initiator(39). YY1 plays a critical role in cardiac development through a number of mechanisms(40, 41). However, the role of YY1 in adult cardiac physiology is poorly understood. YY1 has been shown to attenuate phenylephrine-induced cardiomyocytes hypertrophy by preventing histone deacetylase 5 (HDAC5) phosphorylation and subsequent exporting out of nuclear(42). HDAC5 acts as a repressor of the cardiac hypertrophy through inhibition of myocyte enhancer factor 2 (MEF2)(43). Here we showed that YY1 is implicated in cardiac energetics enhancement in response to exercise and pressure overload. Indeed, knocking down of YY1 in cardiomyocytes resulted in blunted PGC-1α upregulation and mitochondrial respiration enhancement by β-adrenergic stimulation. Therefore, our study revealed a new role of YY1 in the heart and suggested that the YY1 activation could be used to screen TrkB agonists for heart failure therapy.

How the BDNF triggered AKT activation promoting YY1 binding to PGC-1α promoter remains to be elucidated. We observed that there was little change in p-mTOR at serine 2448 and p-TSC2 at threonine 1462 in cTrkB KO mice subjected to exercise or TAC. However, because there could be multiple phosphorylation sites on mTOR or TSC2 by AKT, it is still quite possible that the action of AKT on YY1 is through either mTOR or TSC2, given the binding of Raptor to YY1 was decreased in cTrkB KO mice and Raptor functions as an adaptor protein to mTOR. The YY1 expression was decreased in cTrkB KO mice subjected to swimming exercise or TAC. Whether AKT-mTOR is involved in YY1 transcription needs to investigate.

Recently it has been found that NTRK gene fusions including either NTRK1, NTRK2 or NTRK3 (encoding the neurotrophin receptors TrkA, TrkB and TrkC, respectively) are oncogenic drivers of various adult and pediatric tumour types, and Trk inhibitors were developed to treat NTRK-fusion positive cancers (44). Our findings suggest that these inhibitors need to be used cautiously in the patients with cardiac dysfunction.

In summary, our work revealed a novel role of cardiac BDNF signaling, and further investigation may yield several clinical applications.

METHODS

Animal models and procedures

Study procedures were approved by the Johns Hopkins University and University of Pittsburgh Animal Care and Use Committees in accordance with National Institutes of Health guidelines. Floxed TrkB mice were generated as reported previously (45) and were kindly provide by Dr. David Ginty at Harvard University. Cardiac-specific TrkB KO mice (cTrkB KO) were generated by crossing with αMyHC-Cre mice (Jackson Lab, Stock # 011038) as we reported previously. There was no difference in cardiac function measured by echocardiography at baseline. WT littermate controls and cTrkB KO mice were subjected to swimming exercise in 32 ˚C water, 90 minutes per session, twice a day for 5 days after one week of training session. TAC procedure was performed as previously described (46). Briefly, Sterile surgery was performed in our dedicated facility. Anesthesia was induced with 3.0% isoflurane, and maintained by ventilator at 2.0% isoflurane. Skin

was shaved and cleaned with povidone-iodine. The chest is entered by a limited incision immediate left to the sternum to expose the mid-thoracic aorta. A 7-0 proline suture tie was placed around the aortic arch between bronchiocephalic artery and left common carotid artery and tightened around a 27 or 26 gauge needle - a common diameter for aortic banding in the mouse. Once the tie was fixed, the needle was removed, and the suture/stenosis remained. The chest was then closed with 6-0 proline suture and 5-0 silk suture. Serial echocardiography were performed in conscious mice (VisualSonics, Vevo 3100) as described previously(47).

Mitochondrial isolation and mitochondrial physiology study

Mitochondria from mouse hearts were isolated as described previously (48). Briefly, mouse hearts were homogenized in isolation solution 75 mM sucrose, 225 mM mannitol, and 1 mM EGTA, pH 7.4, with 0.1mg/ml proteinase. The proteinase was neutralized with 3 volume of isolation solution containing 0.2% fatty acid–free BSA (Sigma-Aldrich). After a first centrifugation (500 *g* for 10 min) to discard unbroken tissue and debris, the supernatant was centrifuged at 10,000 *g* for 10 min to sediment the mitochondria, which were washed twice thereafter by centrifugation at 7,700 *g* for 5 min each, the first one with isolation solution in presence of BSA, and the second in absence of BSA.

In brief, mitochondria were assayed in polyethyleneimine-coated XF96 plates using the Seahorse XF system (Seahorse Bioscience) as previosly described (49). After removing the solution of polyethyleneimine, the equivalent of 5–15 µg mitochondrial protein was transferred to each well. The status of the different complexes of the respiratory chain was evaluated with substrates of Complex I (5 mmol/L

glutamate/malate), Complex II (5 mmol/L succinate and 1 μ mol/L rotenone) and Complex IV (0.5 mmol/L N,N,N,N-tetramethyl-p-phenylenediamine [TMPD] and 3 mmol/L sodium ascorbate). Maximal respiratory capacity was analyzed in the presence of 1 mmol/L ADP and 50 μmol/L dinitrophenol.

Mitochondrial DNA copy number and mitochondrial protein level assessment

Mitochondrial DNA and genomic DNA were isolated from mouse hearts using DNeasy Blood & Tissue Kits (Qiagen) according to the manufacturer's instructions. MitoDNA copy number was assessed with Mitochondrially Encoded NADH:Ubiquinone Oxidoreductase Core Subunit 2, (MT-ND2), or Mitochondrially Encoded ATP Synthase Membrane Subunit 6, (MT-ATP6)/genomic DNA (18s RNA genes) ratio as described(50). The Taqman primers were obtained from Thermofisher Scientifics (MT-ATP6: Mm03649417_g1, MT-ND2: Mm04225288_s1, 18 sRNA gene: Hs99999901_s1). Mitochondrial proteins level was evaluated by Western Blot using OXPHOS cocktail antibodies (Abcam, #ab110413).

Cardiac myocytes studies

Neonatal rat cardiac myocytes (NRCMs) were freshly isolated as described previously(47). Briefly, the hearts were quickly removed from one to three days old Sprague Dawley neonates and immersed into chilled KH buffer (pH 7.5) containing: NaCl 140mM, KC1 4.8mM, MgSO4-7H2O 1.2mM, dextrose 12.5mM, NaHCO3 4mM, NaH2PO4 1.2mM, and HEPES 10mM. The ventricles were cut into 1-2mm pieces and the cardiac myocytes isolation was achieved by digestion with 0.04% trypsin and type II collagenase (Worthington #LS004176) 0.4mg/ml in KH buffer at 37˚C. The digestion was

terminated by DMEM containing 10% fetal bovine serum (FBS). Non-cardiomyocyte cells were removed by rapid attachment (90 minutes incubation in culture dishes). Cardiomyocytes were plated at the density of 2X105/ml in DMEM containing 10%FBS and 0.1mM BrdU to prevent the growth of fibroblasts. 24 hours after cells plating, the medium was changed to serum free DMEM containing 0.1% Insulin-transferrin-selenium (Thermo Fisher Scientifics).

Mitochondrial bioenergetics measurements in cutured cardiac myocytes

Oxygen consumption rate (OCR) was measured in NRCMs transfected with control siRNA, TrkB siRNA or YY1 siRNA using the Seahorse XF system (Seahorse Bioscience) as described previously(51). Basal OCR in each well was measured, followed by serial treatment with FCCP (7.5 µmol/L) and rotenone (2 µmol/L). After completion, viability was assessed by crystal violet (CV) staining, and OCR normalized to cell number. Each experiment was repeated to ensure reproducibility, and the data presented are technical replicates (N = 8) of a single representative study.

Western blot, co-immunoprecipitation

Protein extracts were prepared in RIPA lysis buffer (Thermo Fisher Scientific) from snap-frozen heart tissues. Protein concentration was measured by BCA assay (Thermo Fisher Scientifics). The protein electrophoresis were performed on 4–12% Bis-Tris NuPage gels (Thermo Fisher Scientifics) or Bio-Rad Mini-PROTEAN® TGX™ Precast Gels. The Bio-Rad Trans-Blot Turbo Transfer System was used for the proteins transfer to nitrocellulose membranes. Secondary antibodies used were from LI-COR Biosciences. The blots were quantified using Image J or LI-COR Image studio Lite.

BDNF antibody was from Alomone Lab (#ANT-010), PGC-1α was from Abcam (#ab106814), and YY1 was from Santa Cruz Biotech (#sc-7341). Antibodies from Cell Signaling Technologies: (TrkB Cat #4603, p-TrkB #4168, Erk #4695, p-Erk #4370, CREB #9197, p-CREB #9198, AMPK #5832, p-AMPK #4185, TSC2 #4308, p-TSC2 #3617, AKT #4691, p-AKT #4060, and Raptor #2280).

Co-immunoprecipitation: YY1 was immunoprecipitated from 500 µg heart lysates (in RIPA buffer) using 0.5 µg YY1 (Santa Cruz Biotech #sc-7341), and 25 µl Dynabeads™ Protein G (Thermo Fisher Scientifics). Rabbit IgG for AKT or mouse IgG for YY1 was used as anegative control. Co-immunoprecipitated Raptor was probed using an antibody from Cell Signaling Technologies (#2280).

NRCMs were transfected with TrkB and YY1 siRNA (Origene # SR506114 and #SR501936) using Lipofectamine™ RNAiMAX Transfection Reagent (Thermo Fisher Scientifics) according to Manufacture's protocol. The plasmid containing YY1 cDNA, pcDNA3.1 HA-YY1 was a gift from Richard Young (Addgene plasmid # 104395). Transfection of YY1 plasmid was achieved with Lipofectamine 3000 (Thermo Fisher Scientifics) according to Manufacture's protocol. Isopreoterenol 10µM was added to NRCMs 24 hours after transfection of siRNA or YY1 plasmid. The duration of isoproterenol incubation was 48 hours.

Chromatin immunoprecipitation assay

Chromatin immunoprecipitation assay (ChIP assay) was performed using SimpleChIP Plus Enzymatic Chromatin IP kit (CST, Cat#9005) according to the manufacturer's instruction. Briefly, approximately $2.5x10^6$ neonatal myocytes were

harvested and fixed with 1% formaldehyde for 10 min. Chromatin was then digested to mononucleosome using micrococcal nuclease(37 °C 20min), followed by sonication using a Bioruptor (Diagenode) with 5 cycles (30 seconds on followed by 30 seconds off). After centrifugation (10,000 × g, 10 min), the supernatant was used for ChIP assay. Each sample will be aliquated separately for use as input DNA in quantitative PCR analysis. The remainder of each sample were incubated with either YY1 antibody (Cell Signaling Technologies, #46395) , rabbit IgG (negative control) or anti-histone 3 antibody (positive control), and Protein A Dynabeads (Thermo Fisher Scientifics) overnight. After extensive wash, the bound DNA was eluted from the protein A Dynabeads and the crosslink was reversed by the incubation with freshly made elution buffer (1% SDS, 0.1 M NaHCO3) and Proteinase K at 65°C for 4 hours. The DNA was extracted and purified with UltraPure™ Phenol:Chloroform:Isoamyl Alcohol (25:24:1, v/v), and was used as PCR template. Quatitative PCRs were performed with primers listed below: 5'-AAG CGT TAC TTC ACT GAG GCA GAG G-3' (forward) and 5'-ACG GCA CACACT CAT GCA GGC AAC C-3' (reverse).

Quantitative RT-PCR

Total RNA was extracted from either NRCMs or snap-frozen heart tissues using TRIzol reagent (Thermo Fisher Scientifics). Reverse transcription was conducted using High-Capacity cDNA Reverse Transcription Kit (Thermo Fisher Scientifics). Taqman primers (Thermo Fisher Scientifics) were used for quantitative RT-PCR analysis: mouse PPARGC1A (Mm01208835_m1), mouse PPARA (Mm00440939_m1), mouse ESRRA (Mm00433143_m1), and mouse TFAM (Mm00447485_m1).

Statistics

Data were compared within the groups using one-way or two-way ANOVA with Tukey's Post Hoc Test using GraphPad Prism version 6.0. Unpaired student's *t* test was used for comparison between two groups. All tests were two-tailed and a P value of less than 0.05 was considered significant. All values are represented as the mean ± SEM.

CONFLICT OF INTEREST

None to report.

ACKNOWLEDGEMENTS

This work was supported by the National Institutes of Health grant K08 HL130604, American Heart Association Innovative Project Award #18IPA34170219, UPMC Competitive Research Fund (Dr. Ning Feng), and Samuel and Emma Winters Foundation (Dr. Manling Zhang). We thank the University of Pittsburgh Rodent Ultrasonography Core and the funding source for the instrument (NIH 1S10OD023684; Advanced High Resolution Rodent Ultrasound Imaging System).

REFERENCES

1. Lear SA, Hu W, Rangarajan S, Gasevic D, Leong D, Iqbal R, et al. The effect of physical activity on mortality and cardiovascular disease in 130 000 people from 17 high-income, middle-income, and low-income countries: the PURE study. *Lancet.* 2017;390(10113):2643-54.
2. Mandsager K, Harb S, Cremer P, Phelan D, Nissen SE, and Jaber W. Association of Cardiorespiratory Fitness With Long-term Mortality Among Adults Undergoing Exercise Treadmill Testing. *JAMA Netw Open.* 2018;1(6):e183605.
3. Stamatakis E, Gale J, Bauman A, Ekelund U, Hamer M, and Ding D. Sitting Time, Physical Activity, and Risk of Mortality in Adults. *J Am Coll Cardiol.* 2019;73(16):2062-72.
4. O'Connor CM, Whellan DJ, Lee KL, Keteyian SJ, Cooper LS, Ellis SJ, et al. Efficacy and safety of exercise training in patients with chronic heart failure: HF-ACTION randomized controlled trial. *JAMA.* 2009;301(14):1439-50.
5. Piepoli MF, Davos C, Francis DP, Coats AJ, and ExTra MC. Exercise training meta-analysis of trials in patients with chronic heart failure (ExTraMATCH). *BMJ.* 2004;328(7433):189.

6. Belardinelli R, Georgiou D, Cianci G, and Purcaro A. Randomized, controlled trial of long-term moderate exercise training in chronic heart failure: effects on functional capacity, quality of life, and clinical outcome. *Circulation.* 1999;99(9):1173-82.
7. Yancy CW, Jessup M, Bozkurt B, Butler J, Casey DE, Jr., Drazner MH, et al. 2013 ACCF/AHA guideline for the management of heart failure: executive summary: a report of the American College of Cardiology Foundation/American Heart Association Task Force on practice guidelines. *Circulation.* 2013;128(16):1810-52.
8. Ponikowski P, Voors AA, Anker SD, Bueno H, Cleland JGF, Coats AJS, et al. 2016 ESC Guidelines for the diagnosis and treatment of acute and chronic heart failure: The Task Force for the diagnosis and treatment of acute and chronic heart failure of the European Society of Cardiology (ESC)Developed with the special contribution of the Heart Failure Association (HFA) of the ESC. *Eur Heart J.* 2016;37(27):2129-200.
9. Marosi K, and Mattson MP. BDNF mediates adaptive brain and body responses to energetic challenges. *Trends Endocrinol Metab.* 2014;25(2):89-98.
10. Kaess BM, Preis SR, Lieb W, Beiser AS, Yang Q, Chen TC, et al. Circulating brain-derived neurotrophic factor concentrations and the risk of cardiovascular disease in the community. *J Am Heart Assoc.* 2015;4(3):e001544.
11. Fukushima A, Kinugawa S, Homma T, Masaki Y, Furihata T, Yokota T, et al. Serum brain-derived neurotropic factor level predicts adverse clinical outcomes in patients with heart failure. *J Card Fail.* 2015;21(4):300-6.
12. Takashio S, Sugiyama S, Yamamuro M, Takahama H, Hayashi T, Sugano Y, et al. Significance of low plasma levels of brain-derived neurotrophic factor in patients with heart failure. *Am J Cardiol.* 2015;116(2):243-9.
13. Bahls M, Konemann S, Markus MRP, Wenzel K, Friedrich N, Nauck M, et al. Brain-derived neurotrophic factor is related with adverse cardiac remodeling and high NTproBNP. *Sci Rep.* 2019;9(1):15421.
14. Feng N, Huke S, Zhu G, Tocchetti CG, Shi S, Aiba T, et al. Constitutive BDNF/TrkB signaling is required for normal cardiac contraction and relaxation. *Proc Natl Acad Sci U S A.* 2015;112(6):1880-5.
15. Okada S, Yokoyama M, Toko H, Tateno K, Moriya J, Shimizu I, et al. Brain-derived neurotrophic factor protects against cardiac dysfunction after myocardial infarction via a central nervous system-mediated pathway. *Arterioscler Thromb Vasc Biol.* 2012;32(8):1902-9.
16. Doehner W, Frenneaux M, and Anker SD. Metabolic impairment in heart failure: the myocardial and systemic perspective. *J Am Coll Cardiol.* 2014;64(13):1388-400.
17. Schilling J, and Kelly DP. The PGC-1 cascade as a therapeutic target for heart failure. *J Mol Cell Cardiol.* 2011;51(4):578-83.
18. Vega RB, Horton JL, and Kelly DP. Maintaining ancient organelles: mitochondrial biogenesis and maturation. *Circ Res.* 2015;116(11):1820-34.
19. Finck BN, Lehman JJ, Leone TC, Welch MJ, Bennett MJ, Kovacs A, et al. The cardiac phenotype induced by PPARalpha overexpression mimics that caused by diabetes mellitus. *J Clin Invest.* 2002;109(1):121-30.
20. Gilde AJ, van der Lee KA, Willemsen PH, Chinetti G, van der Leij FR, van der Vusse GJ, et al. Peroxisome proliferator-activated receptor (PPAR) alpha and PPARbeta/delta, but not PPARgamma, modulate the expression of genes involved in cardiac lipid metabolism. *Circ Res.* 2003;92(5):518-24.
21. Huss JM, and Kelly DP. Nuclear receptor signaling and cardiac energetics. *Circ Res.* 2004;95(6):568-78.

22. Cheng A, Wan R, Yang JL, Kamimura N, Son TG, Ouyang X, et al. Involvement of PGC-1alpha in the formation and maintenance of neuronal dendritic spines. *Nat Commun.* 2012;3:1250.
23. Matthews VB, Astrom MB, Chan MH, Bruce CR, Krabbe KS, Prelovsek O, et al. Brain-derived neurotrophic factor is produced by skeletal muscle cells in response to contraction and enhances fat oxidation via activation of AMP-activated protein kinase. *Diabetologia.* 2009;52(7):1409-18.
24. Cunningham JT, Rodgers JT, Arlow DH, Vazquez F, Mootha VK, and Puigserver P. mTOR controls mitochondrial oxidative function through a YY1-PGC-1alpha transcriptional complex. *Nature.* 2007;450(7170):736-40.
25. Dibble CC, and Cantley LC. Regulation of mTORC1 by PI3K signaling. *Trends Cell Biol.* 2015;25(9):545-55.
26. Hyde-DeRuyscher RP, Jennings E, and Shenk T. DNA binding sites for the transcriptional activator/repressor YY1. *Nucleic Acids Res.* 1995;23(21):4457-65.
27. Vega RB, Konhilas JP, Kelly DP, and Leinwand LA. Molecular Mechanisms Underlying Cardiac Adaptation to Exercise. *Cell Metab.* 2017;25(5):1012-26.
28. O'Neill BT, Kim J, Wende AR, Theobald HA, Tuinei J, Buchanan J, et al. A conserved role for phosphatidylinositol 3-kinase but not Akt signaling in mitochondrial adaptations that accompany physiological cardiac hypertrophy. *Cell Metab.* 2007;6(4):294-306.
29. Riehle C, Wende AR, Zhu Y, Oliveira KJ, Pereira RO, Jaishy BP, et al. Insulin receptor substrates are essential for the bioenergetic and hypertrophic response of the heart to exercise training. *Mol Cell Biol.* 2014;34(18):3450-60.
30. Jang SW, Liu X, Yepes M, Shepherd KR, Miller GW, Liu Y, et al. A selective TrkB agonist with potent neurotrophic activities by 7,8-dihydroxyflavone. *Proc Natl Acad Sci U S A.* 2010;107(6):2687-92.
31. Massa SM, Yang T, Xie Y, Shi J, Bilgen M, Joyce JN, et al. Small molecule BDNF mimetics activate TrkB signaling and prevent neuronal degeneration in rodents. *J Clin Invest.* 2010;120(5):1774-85.
32. Wong AW, Giuffrida L, Wood R, Peckham H, Gonsalvez D, Murray SS, et al. TDP6, a brain-derived neurotrophic factor-based trkB peptide mimetic, promotes oligodendrocyte myelination. *Mol Cell Neurosci.* 2014;63:132-40.
33. Donovan MJ, Lin MI, Wiegn P, Ringstedt T, Kraemer R, Hahn R, et al. Brain derived neurotrophic factor is an endothelial cell survival factor required for intramyocardial vessel stabilization. *Development.* 2000;127(21):4531-40.
34. Miranda M, Morici JF, Zanoni MB, and Bekinschtein P. Brain-Derived Neurotrophic Factor: A Key Molecule for Memory in the Healthy and the Pathological Brain. *Front Cell Neurosci.* 2019;13:363.
35. Martinowich K, Hattori D, Wu H, Fouse S, He F, Hu Y, et al. DNA methylation-related chromatin remodeling in activity-dependent BDNF gene regulation. *Science.* 2003;302(5646):890-3.
36. Klein ME, Lioy DT, Ma L, Impey S, Mandel G, and Goodman RH. Homeostatic regulation of MeCP2 expression by a CREB-induced microRNA. *Nat Neurosci.* 2007;10(12):1513-4.
37. Mayer SC, Gilsbach R, Preissl S, Monroy Ordonez EB, Schnick T, Beetz N, et al. Adrenergic Repression of the Epigenetic Reader MeCP2 Facilitates Cardiac Adaptation in Chronic Heart Failure. *Circ Res.* 2015;117(7):622-33.
38. Ucar A, Gupta SK, Fiedler J, Erikci E, Kardasinski M, Batkai S, et al. The miRNA-212/132 family regulates both cardiac hypertrophy and cardiomyocyte autophagy. *Nat Commun.* 2012;3:1078.
39. Gordon S, Akopyan G, Garban H, and Bonavida B. Transcription factor YY1: structure, function, and therapeutic implications in cancer biology. *Oncogene.* 2006;25(8):1125-42.
40. Fang S, Li J, Xiao Y, Lee M, Guo L, Han W, et al. Tet inactivation disrupts YY1 binding and long-range chromatin interactions during embryonic heart development. *Nat Commun.* 2019;10(1):4297.
41. Gregoire S, Karra R, Passer D, Deutsch MA, Krane M, Feistritzer R, et al. Essential and unexpected role of Yin Yang 1 to promote mesodermal cardiac differentiation. *Circ Res.* 2013;112(6):900-10.

42. Sucharov CC, Dockstader K, and McKinsey TA. YY1 protects cardiac myocytes from pathologic hypertrophy by interacting with HDAC5. *Mol Biol Cell.* 2008;19(10):4141-53.
43. Zhang CL, McKinsey TA, Chang S, Antos CL, Hill JA, and Olson EN. Class II histone deacetylases act as signal-responsive repressors of cardiac hypertrophy. *Cell.* 2002;110(4):479-88.
44. Cocco E, Scaltriti M, and Drilon A. NTRK fusion-positive cancers and TRK inhibitor therapy. *Nat Rev Clin Oncol.* 2018;15(12):731-47.
45. Liu Y, Rutlin M, Huang S, Barrick CA, Wang F, Jones KR, et al. Sexually dimorphic BDNF signaling directs sensory innervation of the mammary gland. *Science.* 2012;338(6112):1357-60.
46. Zhang M, Takimoto E, Lee DI, Santos CX, Nakamura T, Hsu S, et al. Pathological cardiac hypertrophy alters intracellular targeting of phosphodiesterase type 5 from nitric oxide synthase-3 to natriuretic peptide signaling. *Circulation.* 2012;126(8):942-51.
47. Zhang M, Takimoto E, Hsu S, Lee DI, Nagayama T, Danner T, et al. Myocardial remodeling is controlled by myocyte-targeted gene regulation of phosphodiesterase type 5. *J Am Coll Cardiol.* 2010;56(24):2021-30.
48. Stanley BA, Sivakumaran V, Shi S, McDonald I, Lloyd D, Watson WH, et al. Thioredoxin reductase-2 is essential for keeping low levels of H(2)O(2) emission from isolated heart mitochondria. *J Biol Chem.* 2011;286(38):33669-77.
49. Tocchetti CG, Caceres V, Stanley BA, Xie C, Shi S, Watson WH, et al. GSH or palmitate preserves mitochondrial energetic/redox balance, preventing mechanical dysfunction in metabolically challenged myocytes/hearts from type 2 diabetic mice. *Diabetes.* 2012;61(12):3094-105.
50. Jiang M, Kauppila TES, Motori E, Li X, Atanassov I, Folz-Donahue K, et al. Increased Total mtDNA Copy Number Cures Male Infertility Despite Unaltered mtDNA Mutation Load. *Cell Metab.* 2017;26(2):429-36 e4.
51. Thapa D, Zhang M, Manning JR, Guimaraes DA, Stoner MW, Lai YC, et al. Loss of GCN5L1 in cardiac cells limits mitochondrial respiratory capacity under hyperglycemic conditions. *Physiol Rep.* 2019;7(8):e14054.

FIGURE LEGENDS

Fig 1. The expression of BDNF and the level of phosphorylated TrkB in mice subjected to swimming exercise or TAC

1A. BDNF expression (n=6) and the level of phosphorylated TrkB (n=4) were increased with swimming exercise. **1B.** In contrast with exercise, the expression of BDNF and

phosphorylated TrkB were decreased in TAC hearts (n=4). **P<0.05, **P<0.01, ***P<0.001*

Fig 2. cTrkB KO mice display exacerbated heart failure progression post TAC

2A. Representative echocardiography and histology of WT and cTrkB KO mice subjected to sham or TAC surgery. **2B.** Compared to WT mice, cTrkB mice showed decreased fractional shortening (WT 40.02±2.7% vs cTrkB KO 23.1±2.1%), increased LV end diastolic dimension (LVEDD, WT 3.29±0.17 mmvs cTrkB KO 4.38±0.13 mm) and LV end systolic dimension (LVESD, WT 2.05±0.19 mm vs cTrkB KO 3.4±0.17 mm). (WT n=22, cTrkB KO n=15). **2C**. Heart weight and lung weight were increased relative to WT controls. (WT n=13, cTrkB KO n=9) **2D.** ANP (Nppa) and BNP (Nppb) were increased in cTrkB KO mice subjected to TAC (n=6). **P<0.05, **P<0.01, ***P<0.001*

Fig 3. PGC-1α and metabolic transcriptional factors expression are decreased in cTrkB KO mice subjected to TAC

3A. The PGC-1α mRNA (Ppargc1a) and protein level were significantly lower in cTrkB KO mice subjected to TAC compared to WT controls (n=6). **3B.** PPARα (Ppara), TFAM, and ERRα (Esrra) mRNA level were further diminished in TAC cTrkB KO hearts. (n=5) **P<0.05, **P<0.01, ***P<0.001*

Fig 4. Mitochondrial proteins, mitoDNA copy numbers, and oxygen consumption rate are decreased in cTrkB KO mice subjected to TAC

4A. OXPHOS cocktail western blot showed that mitochondrial proteins including NDUFB8 (complex I), SDHB (complex II), UQCRC2 (complex III), ATP5A (complex IV), and COXII (complex V) were decreased in cTrkB KO mice, compared to WT controls (n=6). **4B.** Mitochondrial DNA copy number, assessed by MT-ND2/18s RNA gene and MT-ATP6/18s RNA gene, was reduced in cTrkB KO mice subjected to TAC (WT n=6, cTrkB n=7). **4C.** oxygen consumption rate of complex II and complex IV were impaired in TAC cTrkB KO hearts relative to WT controls. (n=6) *$^{*}P<0.05$, $^{**}P<0.01$, $^{***}P<0.001$*

Fig 5. BDNF induces cardiac PGC-1α expression through AKT-Raptor-YY1 signaling

5A. The expression of YY1 and the level of phosphorylated AKT were elevated in WT mice responding to TAC, but the elevation was blunted in cTrkB KO mice (n=8). **5B.** YY1 was immunoprecipitated from TAC WT and cTrKB KO heart lysates. Co-immunoprecipitation study showed the binding of Raptor to YY1 was attenuated in cTrkB KO mice subjected to TAC, compared to WT controls (n=4). *$^{*}P<0.05$, $^{**}P<0.01$, $^{***}P<0.001$*

Fig 6. YY1 mediates the BDNF-induced PGC-1α expression in NRCMs

6A. Isoproterenol (10μM) induced BDNF expression in NRCMs. **6B.** P-AKT, YY1 and PGC-1α expression were increased with isoproterenol stimulation, and the upregulation was attenuated in TrkB siRNA transfected NRCMs (n=4). **6C**. Chromatin Immunoprecipitation Assay demonstrated the binding of YY1 to PGC-1 promoter was significantly decreased in NRCMs with TrkB knockdown and the incubation of isoproterenol (n=4). **6D and 6E.** YY1 knockdown decreased PGC-1α expression, and the overexpression of YY1 in NRCMs recovered the downregulation of PGC-1α expression in NRCMs with TrkB knockdown (n=4).* *P<0.05, **P<0.01, ***P<0.001*

Fig 7. NRCMs with TrkB or YY1 knockdown display impaired oxidative respiratory function

7A. While there is no significant difference in oxidative respiratory capacity without isoproterenol stimulation between control and NRCMs with TrkB knockdown, but the basal respiratory function was significantly decreased with TrkB knockdown in the presence of isoproterenol (n=8). **7B.** NRCMs transfected with YY1 displayed both impaired basal and maximum respiration, at both baseline and with isoproterenol incubation (n=8). **P<0.05, **P<0.01, ***P<0.001*

Fig 8. The upregulation of PGC-1α and metabolic transcription factors responding to exercise is blunted in cTrkB KO mice

8A. The PGC-1α mRNA (Ppargc1a) and protein level were increased with swimming exercise, but the upregulation was blunted in cTrkB KO mice. **8B**. Similarly, the

upregulation of PPARα (PparaA), TFAM, and ERRα (Esrra) were attenuated in cTrkB KO mice (n=6). **8C.** The expression of YY1 and the level of phosphorylated AKT were elevated in WT mice responding to exercise, but the elevation was blunted in cTrkB KO mice (n=8). **P<0.05, **P<0.01, ***P<0.001*

SUPPLEMENTAL DATA

Fig S1. Female cTrkB KO mice show accelerated heart failure progression post-TAC

Fig S1. Compared to WT mice, female cTrkB mice showed decreased fractional shortening (WT 44.6±3.4% vs cTrkB KO 27.7±4.4%, P=0.0062), increased LV end diastolic dimension (LVEDD, WT 2.94±0.16 mm vs cTrkB KO 3.8±0.2 mm P=0.0006) and LV end systolic dimension (LVESD, WT 1.7±0.2 mm vs cTrkB KO 2.8±0.3 mm, P=0.0002). (WT n=11, cTrkB KO n=7). ***P<0.01*

Fig S2. Complex I oxygen consumption rate is preserved in cTrkB KO mice subjected to TAC

There is no difference in complex I respiration between WT and cTrkB KO mice after TAC. (n=6).

Fig S3. Erk, CREB, AMPK mTOR or TSC2 signaling pathways in WT or cTrkB KO mice subjected to TAC

A. There was no change in phosphorylated or total Erk, CREB AMPK levels in cTrkB KO mice subjected to TAC. **B.** Chromatin immunoprecipitation Assay showed there was no difference in the binding of CREB to PGC-1α promoter between TAC WT and cTrkB KO mice. C. There was no change in phosphorylated or total mTOR and TSC2 levels in cTrkB KO mice. (n=4)

Fig S4. The efficiency of TrkB knockdown with siRNA in NRCMs

Quantitative RT-PCR showed TrkB mRNA was decreased by 75% with siRNA in NRCMs.

Fig S5. Erk, CREB, AMPK, mTOR or TSC2 signaling pathways in WT or cTrkB KO mice subjected to swimming exercise

There is no difference in the level of phosphorylated or total Erk, CREB, AMPK, mTOR or TSC2 between WT and cTrkB KO mice subjected to exercise.

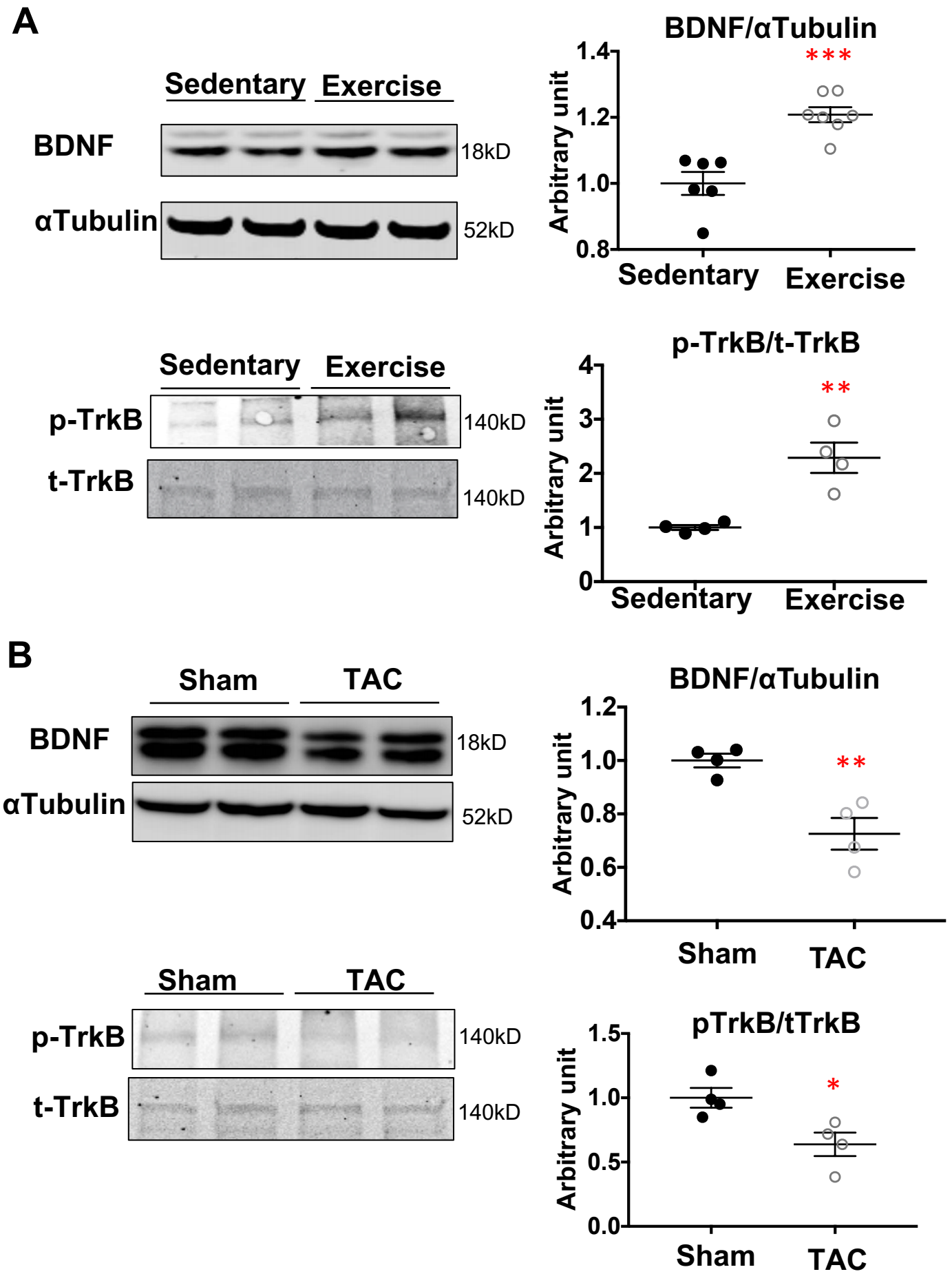

Fig 1

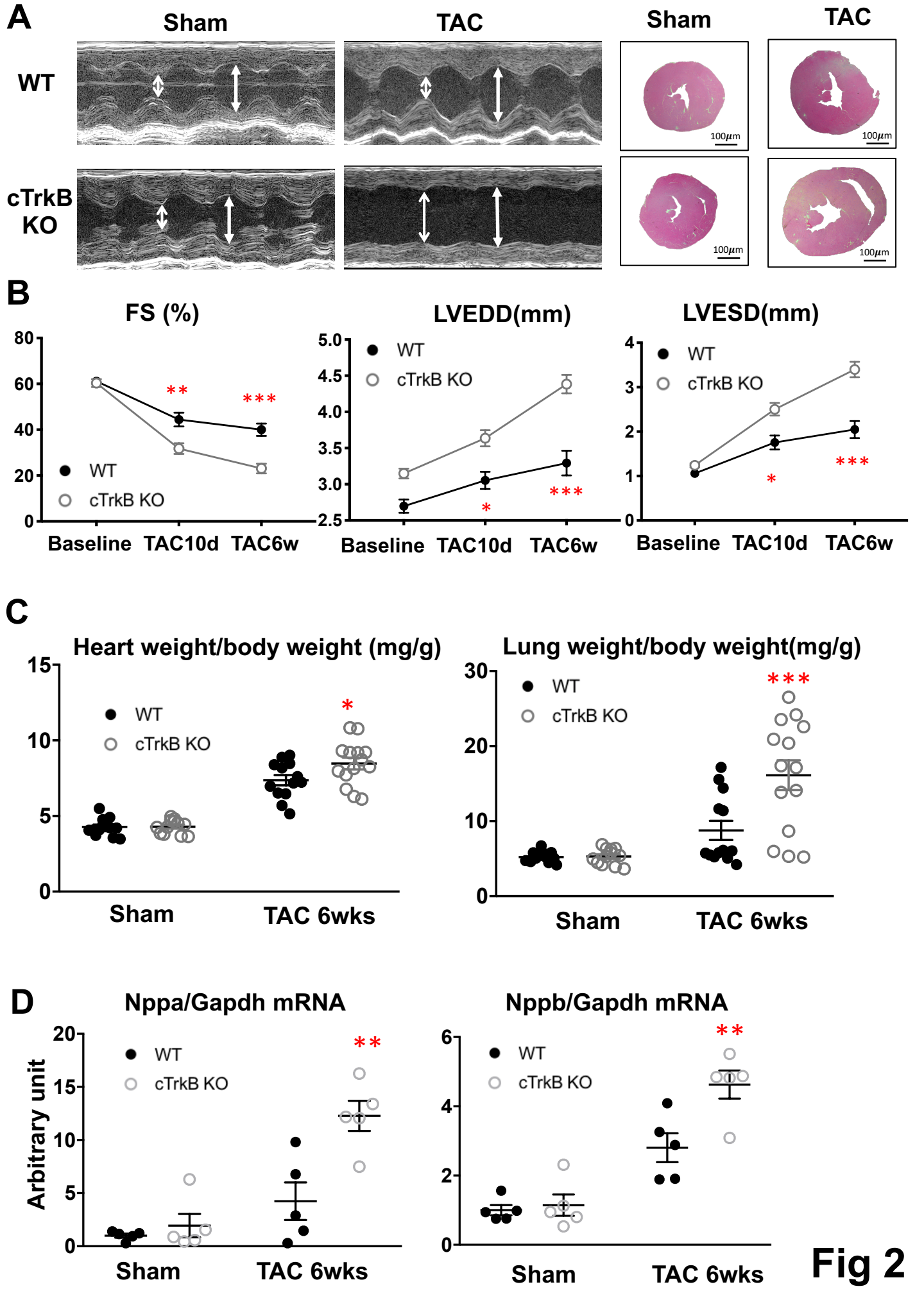

Fig 2

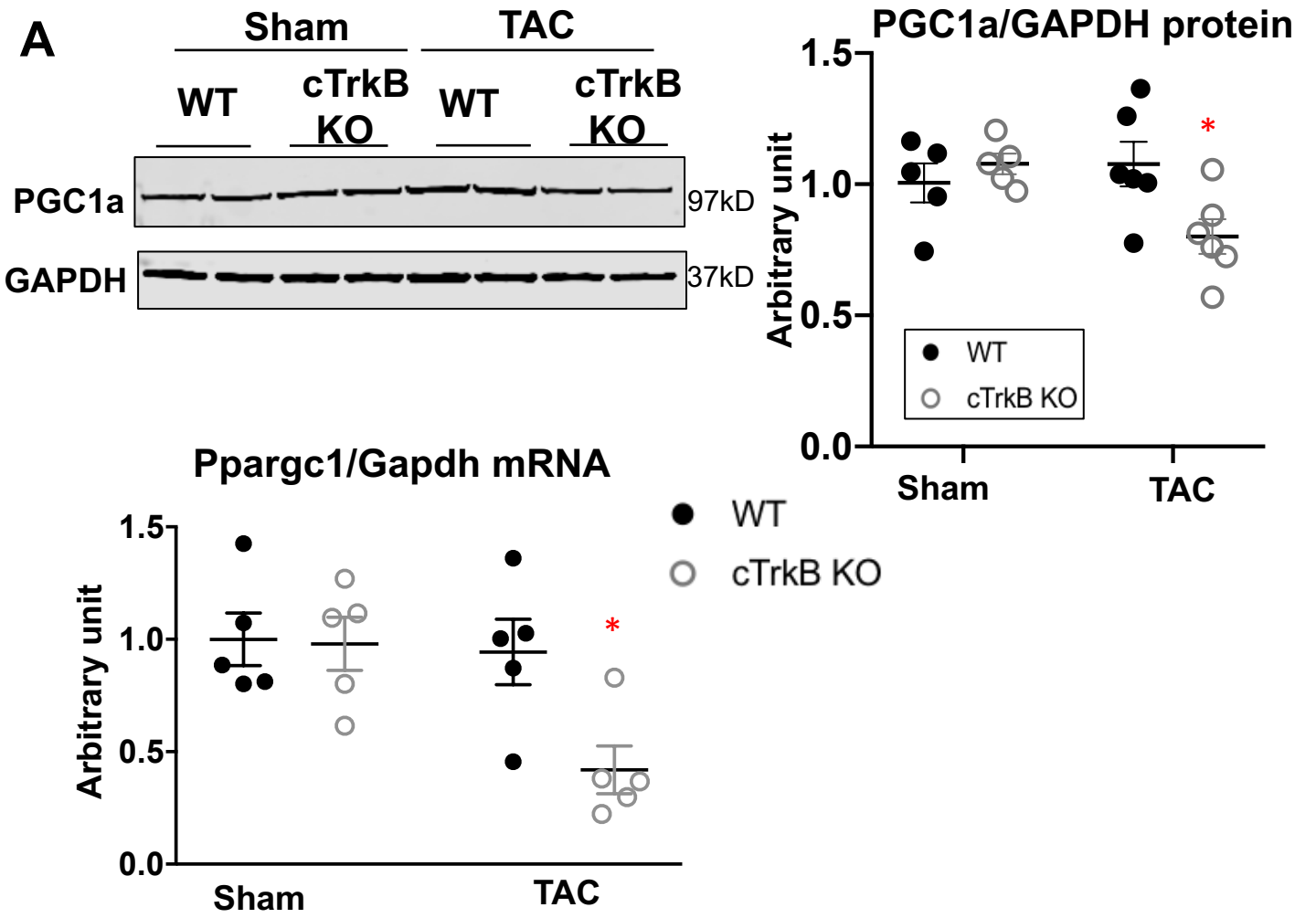

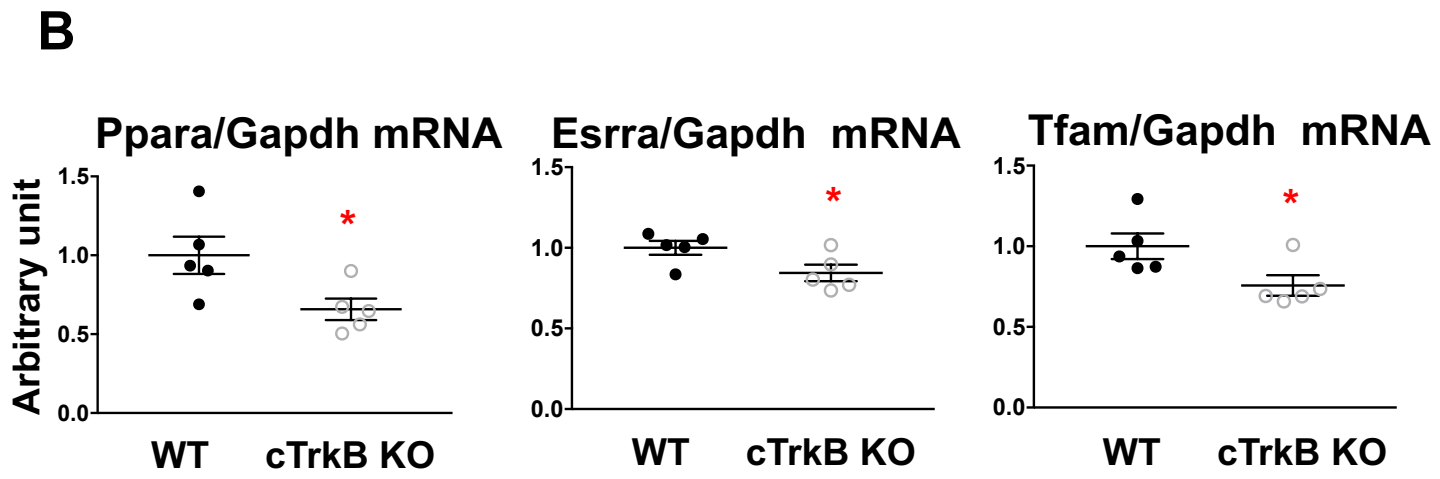

Fig 3

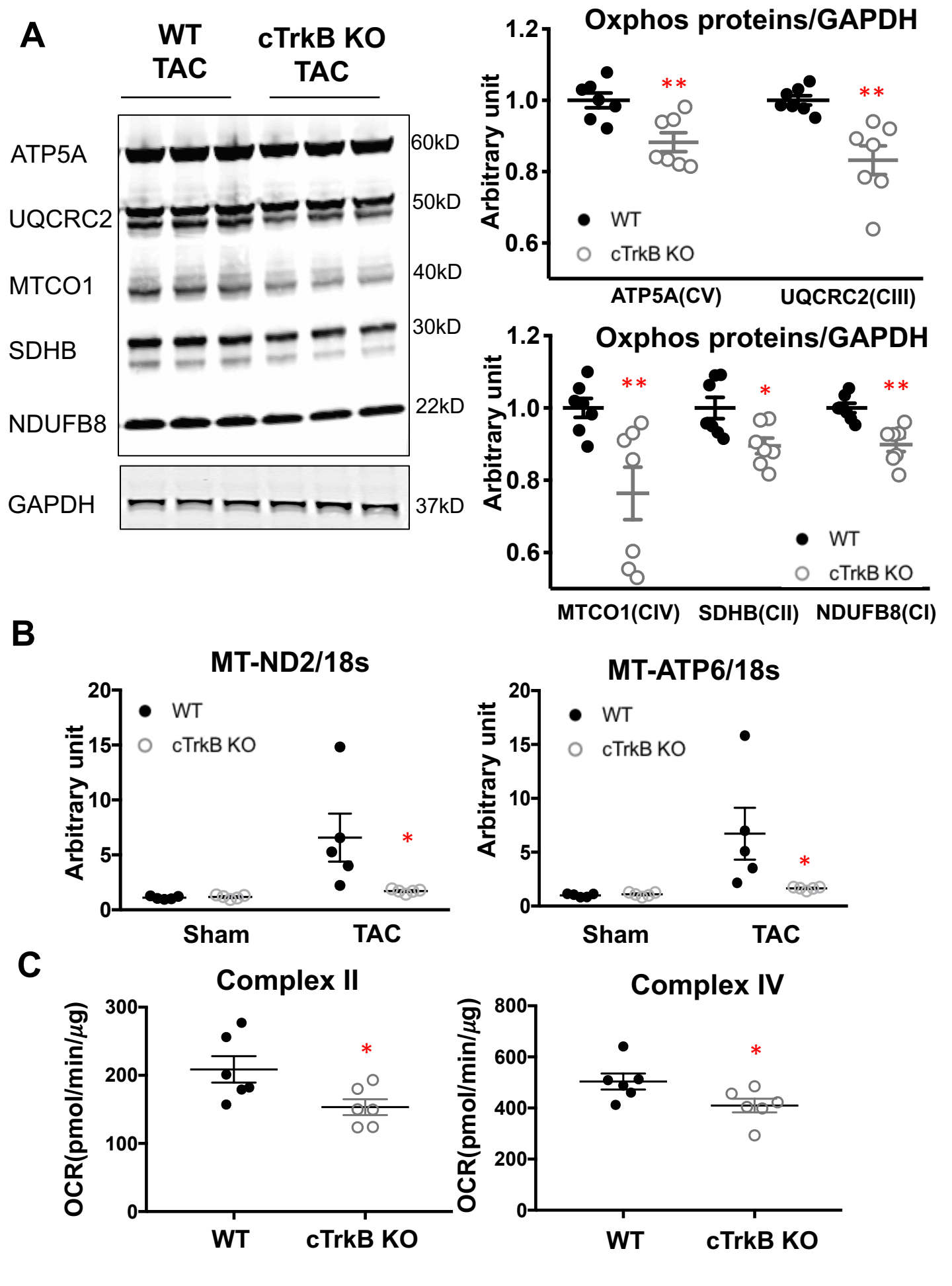

Fig 4

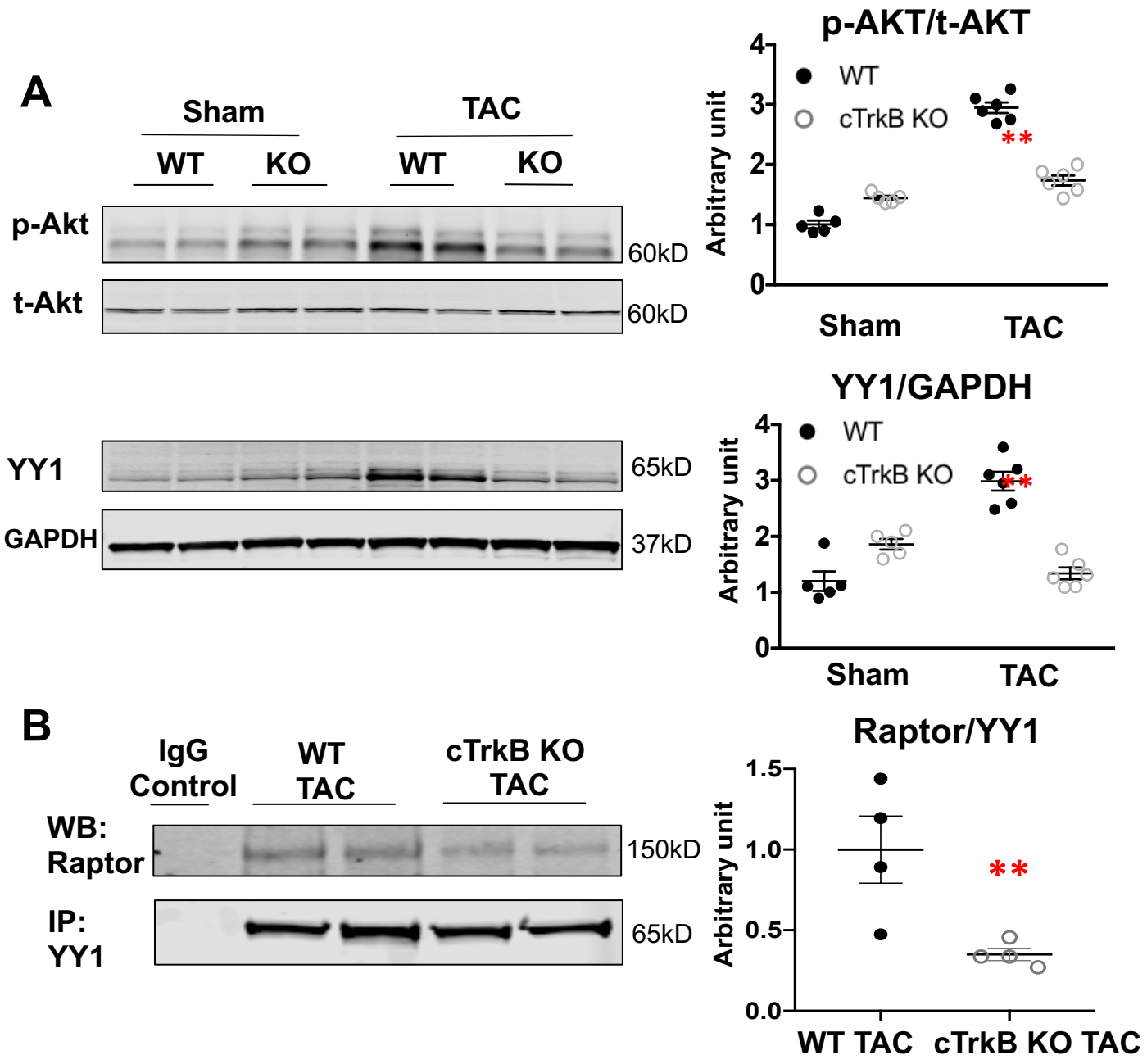

Fig 5

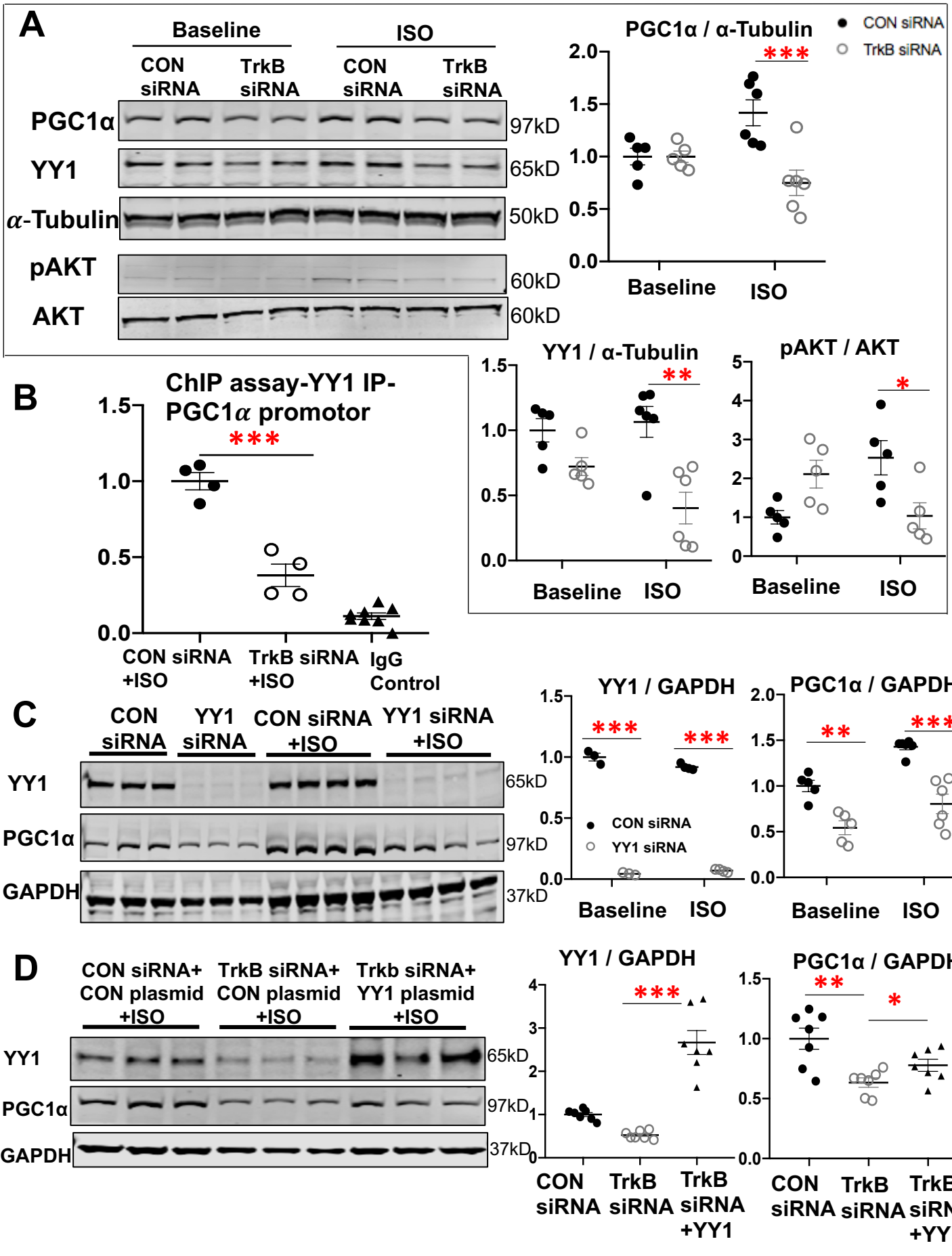

Fig 6

A

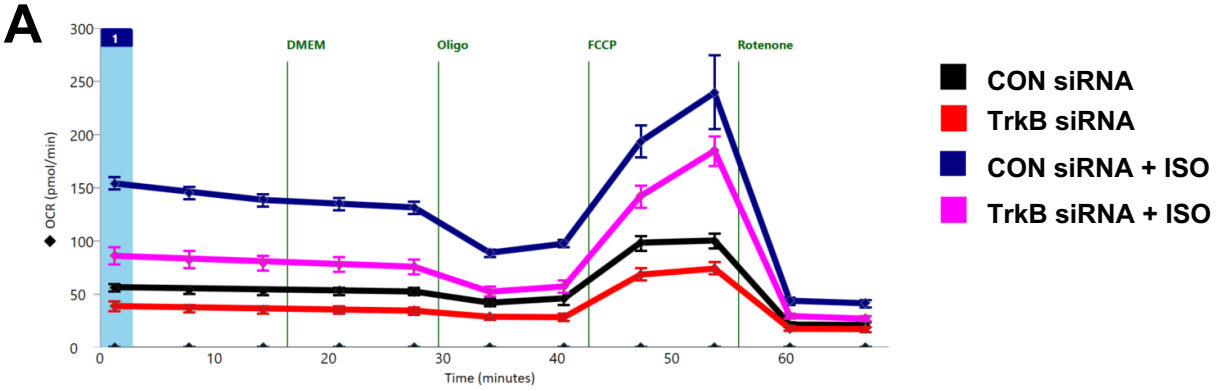

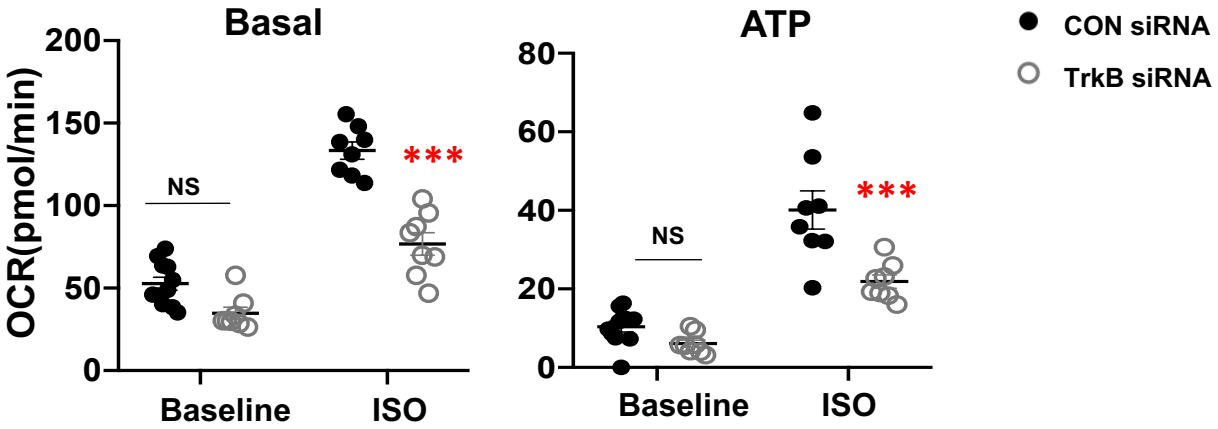

B

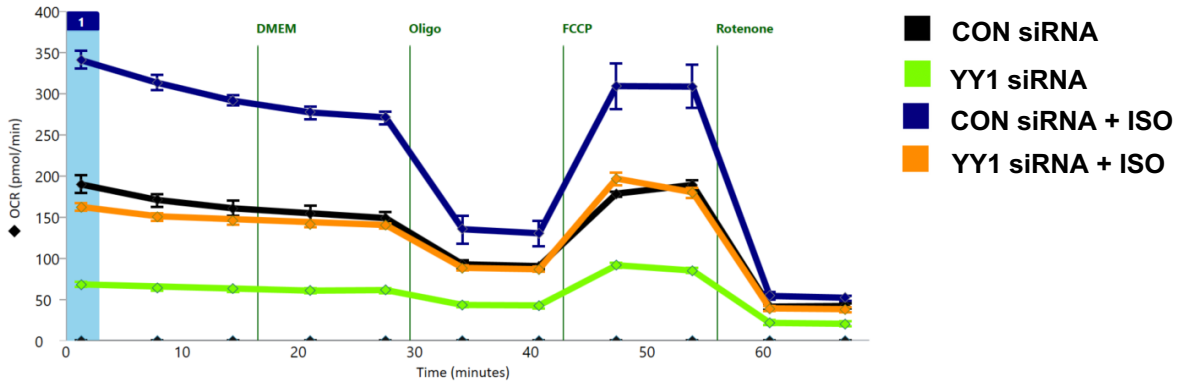

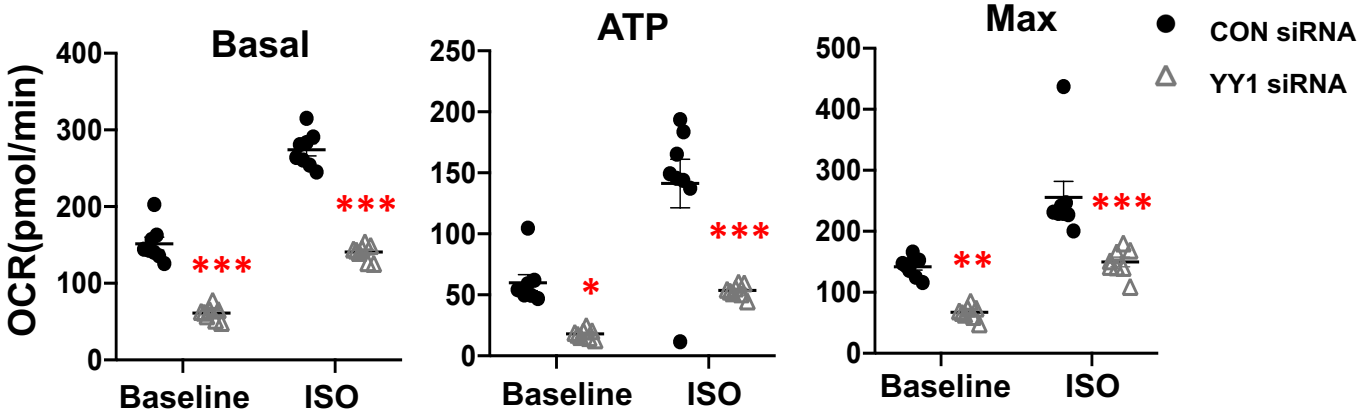

Fig 7

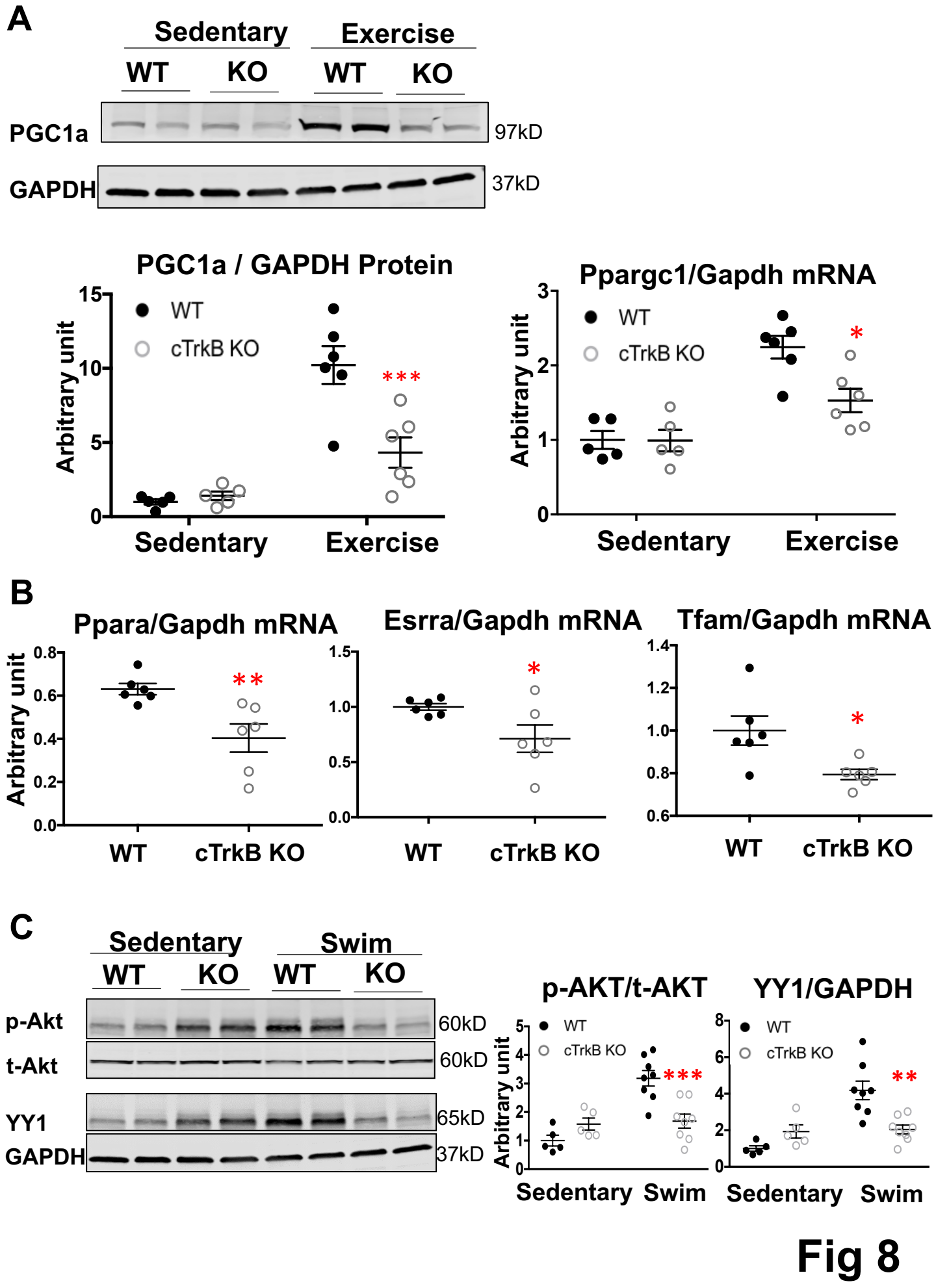

Fig 8

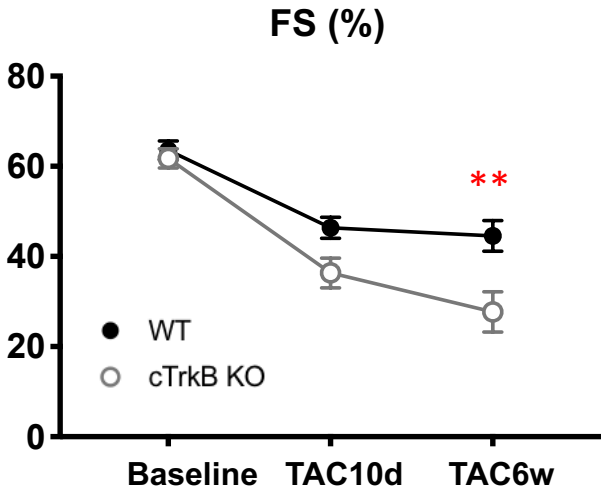

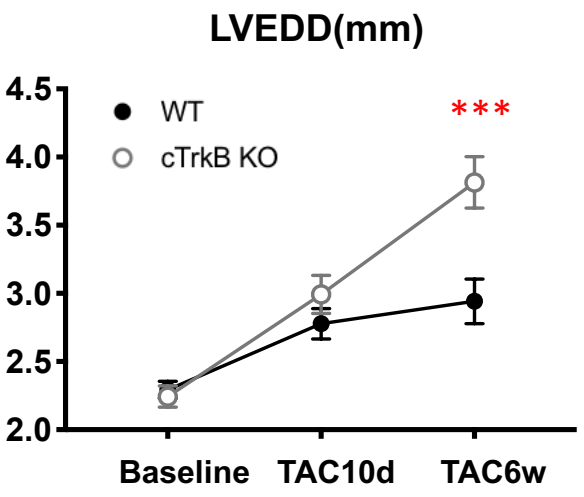

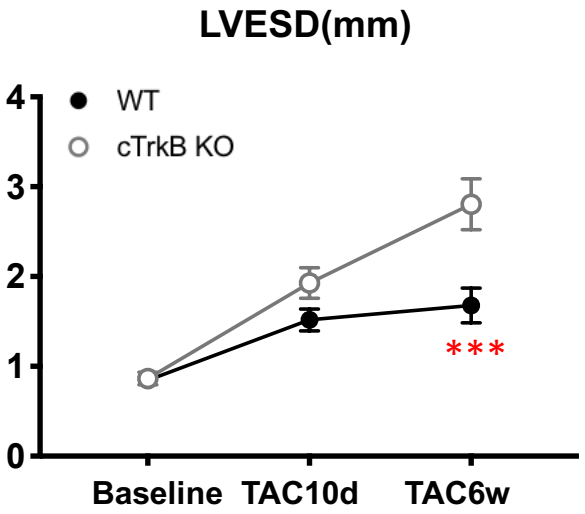

Fig S1

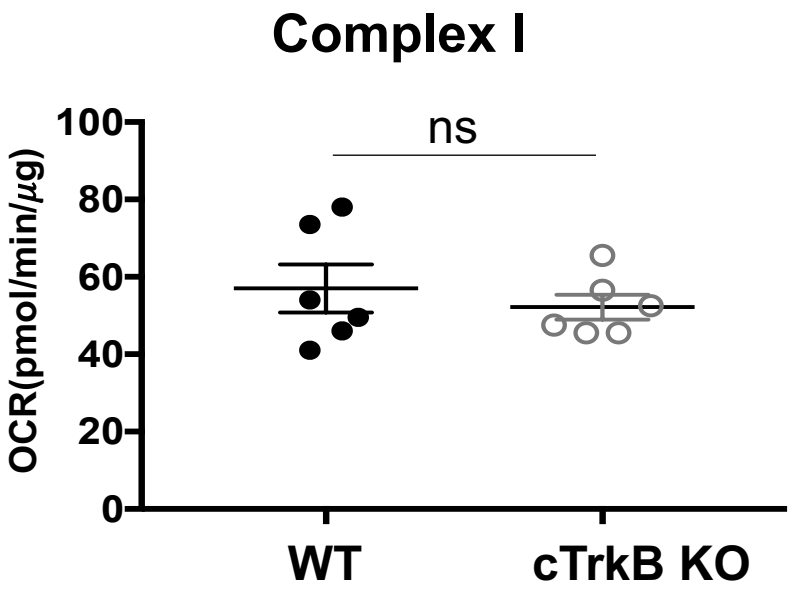

Fig S2

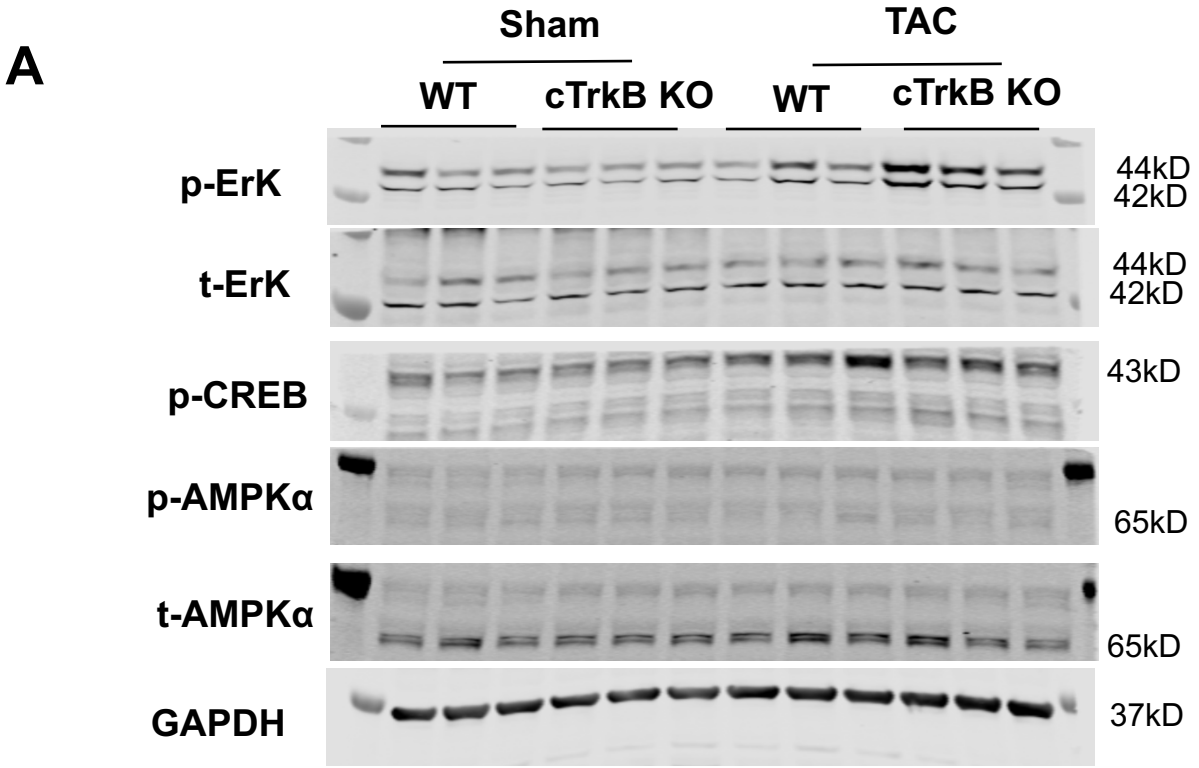

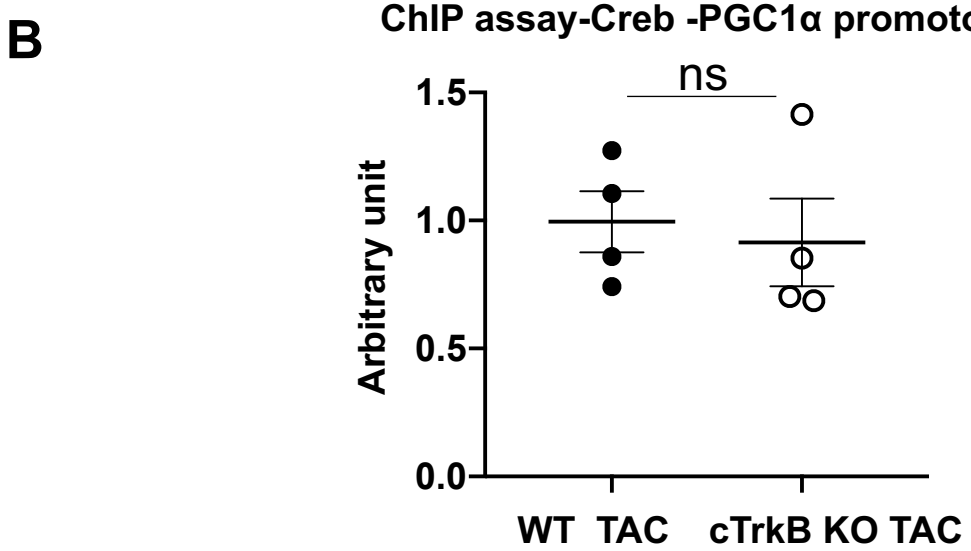

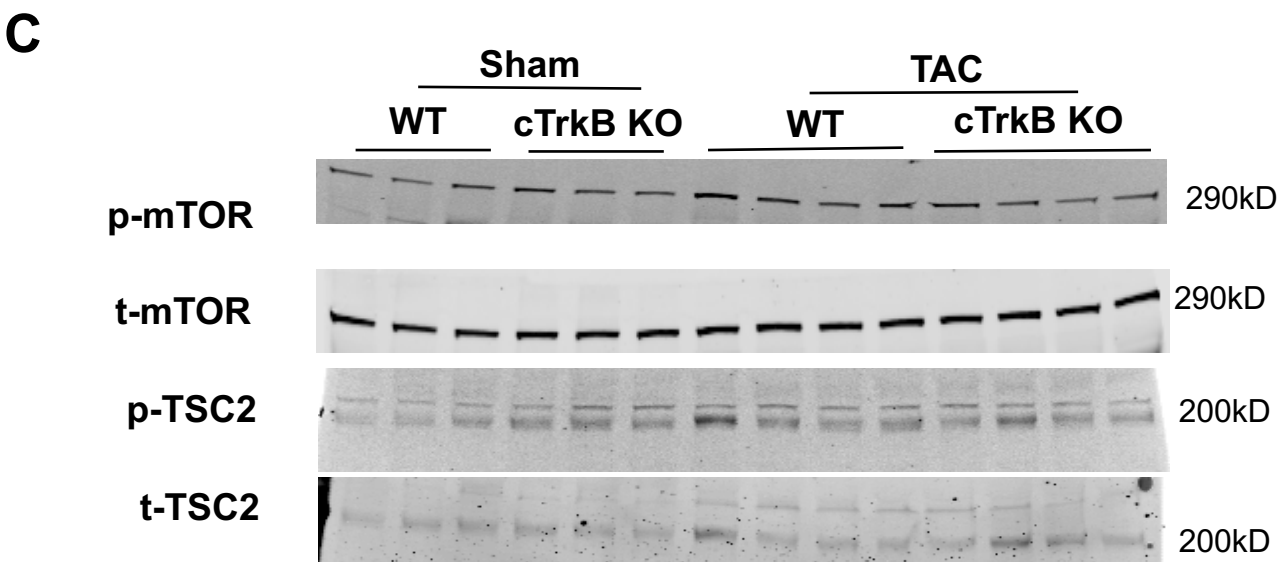

Fig S3

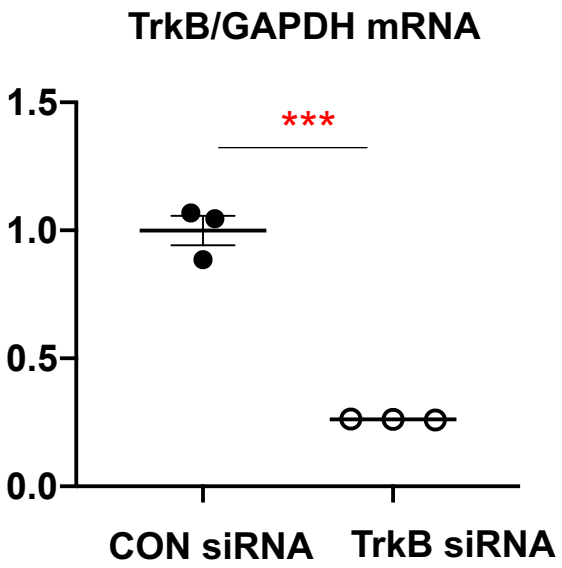

Fig S4

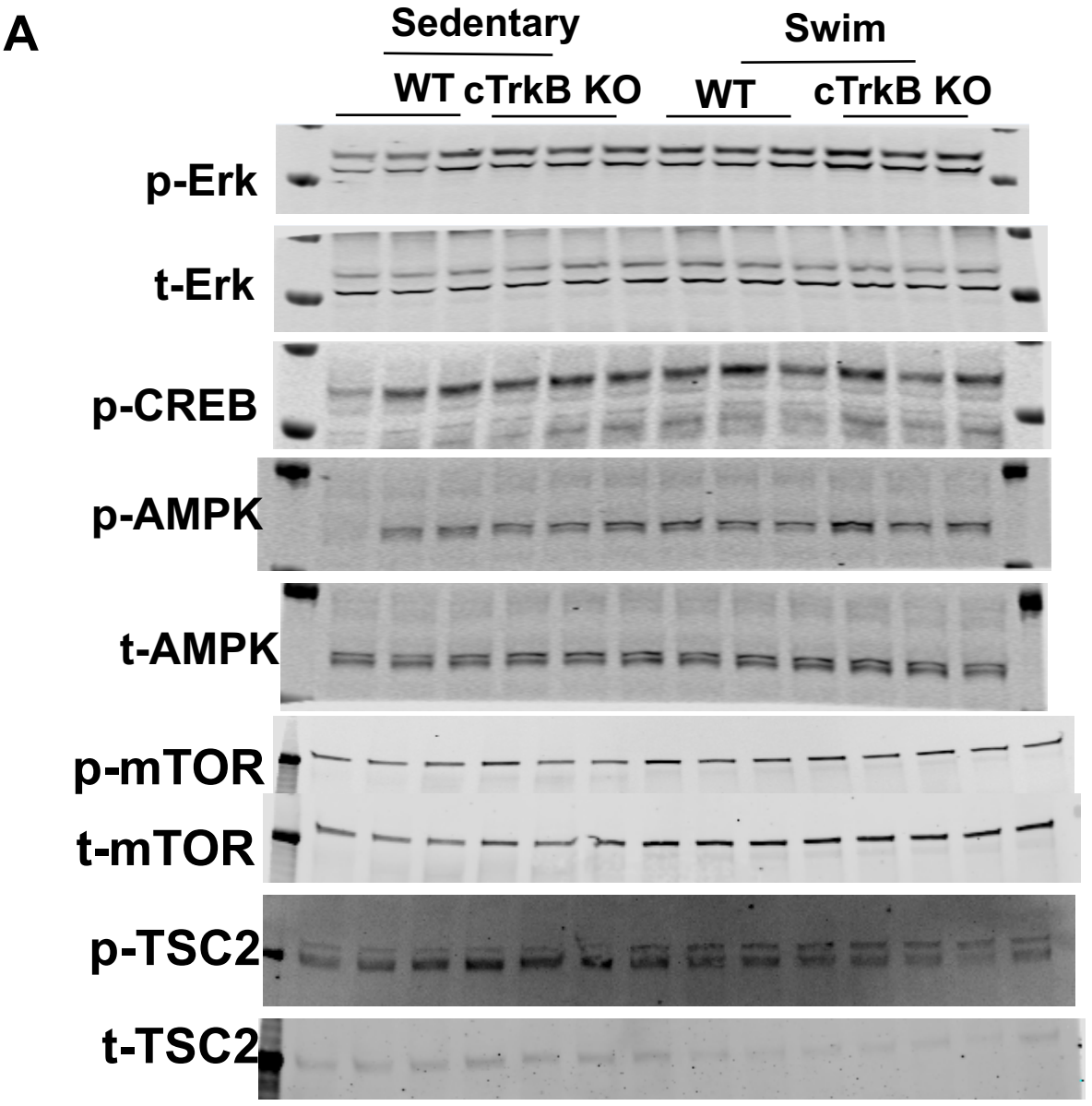

Fig S5